National Conference on Wind Tunnel Testing
12-14 March 2009, Bangalore

Flow field study on a 65-deg blunted delta wing

B. Nath[1], S. Das[2] and J.K. Prasad[3]
1. NTAF, National Aerospace Laboratories, Bangalore, buddhadebnath@gmail.com
2. Department of Space Engineering and Rocketry, BIT, Mesra, Ranchi, sudipdas@bitmesra.ac.in
3. .Department of Space Engineering and Rocketry, BIT, Mesra, Ranchi, jkprasad.1@gmail.com

ABSTRACT

The distinguishing feature of the delta wing is characterized by leading edge vortices which cause highly nonlinear forces and moments. At a sufficiently high angle of attack these vortices breakdown over the surface and introduce an additional transient in the aerodynamics. The understanding of aircraft aerodynamics with separated flows over the wing will permit design for increased maneuverability in future aerospace vehicles. Here, experimental and numerical investigations are carried out to obtain the complex flow field features on a 65° delta wing. Experiments are conducted at a nominal speed of 20m/s and Reynolds number of 2×10^5 at low subsonic wind tunnel facility. The qualitative techniques of oil flow visualization and tuft flow visualization and quantitative techniques of static pressure measurements have been used to observe various features of flow field. The angle of attack and side slip angle were varied in the range from 5° to 40° and 0° to 20° respectively. The effect of angle of attack, side slip, and speed variation on surface pressure and the effect of angle of attack on approximate vortex breakdown location were captured. Three dimensional numerical simulation were performed using the commercial software FLUENT over the delta wing. At the high angle of attack the major part of the flow over the wing is affected by vortex breakdown and vortex breakdown is asymmetric in nature. Side slip causes a strong asymmetry on the surface flow and pressures.

NOMENCLATURE

α	Angle of attack(AoA)
β	Angle of side (AoS)
Λ	Sweep angle
b	Wing span
Cp	Static Pressure coefficient
U	Velocity
s	Semi span
c	Root chord
Re_c	Reynolds number based on chord
x/c	Non – dimensional coordinates along the root chord
y/s	Non – dimensional coordinates along the span

X_b/c	Non-dimensional location of vortex breakdown along the root chord
t	Thickness of model
R	Model bluntness
Subscripts	
∞	Free stream

INTRODUCTION

Study of flow field on the Delta wings has been of interest to researchers due to its application towards design of highly maneuverable aircrafts. The development of highly maneuverable aircraft, missiles, and reusable launch vehicle has generated interest in the study of delta wings due to possible advantage of better stability and control characteristics. The flow over such wings generates separation induced leading edge vortex flow which will depends on various factors like slenderness, sweep angle, shape of leading edge, angle of attack, free stream velocity, Reynolds number etc. At high angles of attack, the onset of flow separation might lead to formation of vortex flow which can have crucial effect on the performance of aircraft. Therefore the details of flow field obtained will be of immense use to the designer. Extensive studies over delta wing having sharp leading edge have been reported. A vortex which is anchored at the origin of leading edge is formed which increases in diameter downstream on the leeward side of the wing. The growth, axial and rotational velocities of vortex will depend on factors like leading edge angle, angle of attack and incoming flow parameters. At high angle of attack, the leading edge core vortex flow disorganizes and leads to vortex breakdown. This will lead to strong fluctuation of the wing surface pressure down stream of the break down point and might lead to buffeting. This phenomenon is likely to deteriorate the aircraft performance, stability and control. Many researchers have reported the investigation made over delta wing adopting experimental and computational approach. Flow over delta wing is reported by Verhaagen and Jobe [1], Verhaagen and Kunst[2], Ahmed et al. [3], Honkan and Andreopoulos [4], Taylor and Gursul [5], Yavuz et al [6], Luckring [7], Yaniktepe and Rockwell [8] and many others adopting experimental and computational techniques. Research carried out to obtain the details of vortex breakdown on delta wing is reported by Lin and Rockwell [9], Francis et al. [10], Erickson [11] and others. In order to control the vortices, various techniques are adopted, as reported by Gutmark and Guillot [12], Gursul et al [13], Wang et al [14], Russel [5]. Studies made to obtain the flow field details adopting PIV, PSP are reported in Ref 16-18.

In the case of Delta wing having sharp leading edge, the separation is fixed. At high angle of attack, this leads to a primary vortex moving downstream. Depending upon leading edge angle and other flow parameters, a secondary vortex is also formed. In general attached flow is observed in the central part of the wing. However in the case of wing having blunt edge, (which is generally found in practice), the flow becomes more complex. The main reason being that the primary separation is no longer affixed at the leading edge and hence the flow will depend on bluntness in addition to other parameters as in the case of wings having sharp leading edge. This added complexity might change the performance appreciably.

In the present investigation, study has been made to obtain the flow field over a typical delta wing having 65° sweep at angles of attack up to 40° and at angles of side slip up to 20°. Flow visualization tests including tuft flow and oil flow, surface pressure measurements at various axial locations were performed. In addition the computation have been adopted to predict the flow field using commercial software FLUENT.

EXPERIMENTAL SETUP

All the experiments have been made using the Subsonic Wind Tunnel at Birla Institute of Technology, Mesra, Ranchi. The tunnel has the test section size of 2ft x 2ft and speed in the range of 10 to 30 m/s. It is an open circuit continuous flow wind tunnel in which air is sucked by the four bladed constant pitch propeller located at the aft section of the tunnel which is driven by a 440 V, 15 HP induction motor. A schematic sketch showing the details of the tunnels is shown in Fig.1. Fig.2 shows the photograph of the tunnel with multi tube water column manometer and pressure sensor box, which was used to record, all the pressure data from the model. During the present investigation, tests have been made at a fixed free stream velocity of 20 m/s. A delta wing having sweep angle (Λ) of 65 deg and having the base width (b) of 166 mm and chord (c) of 168 mm was fabricated using Rapid Prototype Machine using a polymer (ABS), for which the coordinates were generated using software CATIA. The model had thickness (t) of 10mm and bluntness (R) of 5mm. Necessary mounting arrangement for changing angle of attack in pitch plane and provision for measurement of static pressure ports were made. The model details are shown in Fig.3. For flow visualization, the technique of tuft flow and oil flow was adopted. A mixture of lamp black, kerosene oil, lubrication oil and oleic acid was sprayed over the model for oil flow visualization. Photographs were taken using a digital camera end of each test run for further analysis. Attempts were also made to capture the unsteady behaviors of flow field through movie camera. For the measurement of static pressure, steel tube having inner diameter of 0.8mm was fixed at different locations on the model. The pressure port was connected to the measuring instrument. The static pressures were measured using multi tube water manometer and as well using pressure pickups. The data were acquired using NI card, LabView, a dedicated DAS for further analysis. The tests were carried at angles of attack up to 40° and at angles of side slip up to 20°. Reynolds number based on chord was 2×10^5. The overall accuracy of pressure measurement is estimated to be better than 5%. Repeatability tests indicate an uncertainty in Cp of ±0.05.

COMPUTATIONAL METHOD

Computations have been made using the commercial software FLUENT available at the Institute. Various turbulence models were attempted and it was found that Spalart-Allmaras (SA) model available with FLUENT software gives the results which are much faster and comparable, compared to other turbulence models. Similar observation is reported by other investigators also. Three-dimensional Coupled solver with implicit formulation is adopted for all the computations. Upwind discretisation scheme for flow as well as transport equations were selected. Residuals were monitored

during the solution progress with convergence criterion of 10^{-5}. In addition the c_l and c_d history were also monitored during the solution. The 3-D computational mesh was prepared using the pre-processor of FLUENT. Tetrahedral cells were created in the region, surrounding the geometry and bounded by a domain which has a minimum influence to the solution of interest. Due to symmetry, only one half of the delta wing was taken. The wing was fixed at a centre location of one of the boundaries of the domain which was assigned as a symmetry boundary. Other boundaries which are very far from the wing were assigned with pressure far field boundary. No slip condition was assigned to all the surfaces of the wing. Typical grid distribution along with the computational domain and boundary condition is shown in Fig.4. A typical number of cells used during the present computation was 3,50,000 which were arrived at after conducting grid convergence tests. All the computations have been made using Pentium IV with RAM of 1 GB. Various details like pressure, velocity, density contours, pressure distributions along x and y direction were obtained for comparison with experimental results.

RESULT AND DISCUSSION

A typical tuft flow observed on the leeward side of the wing at α=20°and β=20° is shown in Fig. 5. A typical oil flow pattern observed on the leeward side of the wing at α=20° is presented on the left side of Fig. 6. Most of the features like axially attached flow in the central part of the model, primary separation line and attachment line, secondary separation line and attachment lines etc could be captured qualitatively. This oil flow pattern is compared with corresponding static pressure coefficient at different x/c is shown in Fig.6. A fairly good correlation is observed between oil flow and static pressure. This is clearly observed that pressure peak is seen always between primary attachment line and secondary separation line but closer to secondary line which is also reported in Ref. [19]. The conical structure of separated flow is also confirmed from the fig. 6. Static pressure distribution at x/c =0.6 in the Fig. 6 clearly indicates the existence of two vortex cores. Such details are obtained at different angle of attack. The vortex breakdown could be clearly seen from the oil flow pattern observed at α=35° in Fig 7. From such photograph obtained at different angle of attack, it is possible to locate the approximate position of vortex break down which will be discussed later. The comparison of the computed oil flow obtained through FLUENT with the experimental result is presented in the Fig. 8 which indicates that qualitative comparison is fairly good.

Measurement of static pressure have been made at different axial location and at different α and β and presented as a pressure coefficient (Cp). The effect of α on pressure distribution on the leeward side of the wing at axial location of x/c =0.5 is presented in Fig 9. It is clearly seen that pressure suction increases with increase in α up to α=30°. However the trend changes at α=35° & 40° due to vortex break down. It is also seen that over all radius of vortex at this axial location increases with increase in α.

After comparing effect of α variation on Cp at different x/c (like Fig 9) and oil flow at different α (like Fig 7), an attempt has been made to predict approximate vortex breakdown location. All the distances were measured by scaling the model from the

photograph of oil flow to its real dimension. At various angles of attack the vortex breaks down location were determined from photograph of oil flow. Fig.10 shows vortex break down location (X_b/c) vs. angle of attack for various sweep angle and bluntness for four Delta wings. (1) Λ=65°, rounded leading edge (present case), Re=2x10^5; (2) Λ=60°, rounded leading edge, Re=2.3x10^6; [Ref.19] (3) Λ=60°, sharp leading edge, Re=2.3x10^6; [Ref.19] (4) Λ=70°, sharp leading edge, Re=0.16x10^6; [Ref.21]. This comparison holds because the vortex break down position is roughly independent of Reynolds number for higher value of Re_c [Ref.19]. In case of present model, vortex break down occur beyond the trailing edge for α<12 deg. The general characteristics in Fig. 10 confirmed that the vortex breakdown location moves upstream over the delta wing, from the trailing edge towards the apex, as α is increased. The comparison with the experiment confirms some general trends. In the one hand, increasing sweep angle for sharp leading edge appears to follow the same slope of vortex breakdown location but the trend is delayed at some high angle of attack range. Similar behavior is observed for round leading edge with 60° and 65° (present case) sweep angle. The slope of the breakdown location evolution with α is same for both results with sharp as well as round leading edges. An increase in sweep angles appears merely to shift the breakdown position downstream without changing its evolution. In the other hand the leading edge shape modifies both the vortex breakdown position and its evolution. Above trends also seen in Ref. [19].

The effect of speed variation on Cp at x/c=0.5 is shown in Fig.11. As speed increases, separation of leading edge promotes which is also observed by Luckring[7].

The effect of β at α=20° on the measured pressure distribution are described in Fig 12. At β (or AoS) =0, magnitude of negative Cp or suction induced by vortices is strong on front part of the wing whereas downstream of this station the suction peak decrease in magnitude and extend in lateral direction .
When delta wing is yawed to 10°, the displacement of vortices shifts the suction peak into the leeward direction. On the leeward wing half a strong reduction of suction peak is observed. The value of the suction is largest on the windward half. When β is increased further to 20°, reduction of suction of the curves continues to occur on leeward wing half. On the wind ward wing half, suction peak is increased up to x/c =0.5 as compared β=10° case, then suction peak is reduces probably due to vortex break down .The suction force on the windward wing half is much higher than that on the opposite half.

Fig. 13 shows effect of β on the leeward surface Cp at x/c =0.5 at α=20°. As just described, the Cp on the leeward surface is strongly affected by β.

Computed results were compared with corresponding experimental results. A typical comparison is presented in Fig 14, which shows the pressure distribution at x/c=0.7, and indicate fairly well in windward side in comparison to leeward side. However the trend seems to be similar. Some more computational results are published in Ref [22].

CONCLUSION

In order to study the complex flow field over a blunt delta wing, experimental and computational study has been made. Experiments consisted of flow visualization and measurement of static pressure on the surface of the delta wing. Experiments conducted at different angles of attack and side slip indicates the presence of vortex and location of vortex break down. The pressure distribution on the leeward surface is strongly affected by β. Computation made using FLUENT shows good comparison with experimental results.

REFERENCES:

[1]. Verhaagen N.G. and Jobe C.E., "Wind tunnel study on a 65-deg Delta Wing at side slip", JOURNAL OF AIRCRAFT , Vol. 40, No. 2, 2003.

[2] Niek G. Verhaagen and Victor F. Kunst, "Topology of the flow on delta wing at side slip", AIAA 2005-60.

[3]. Ahmad Z. Al-Garni, Farooq Saeed, Abdullah M.Al-Garni, Ayman Abdullah, Ayman Kassem, "Experimental and Numerical Investigation of 65-deg delta and 65/40 – deg double delta wings", AIAA paper 2006-0063.

[4] A.Honkan and J. Andreopoulos, "Instantaneous three dimensional vorticity measurements in vertical flow over a delta wing", AIAA Journal, Vol.35, No.10, 1997.

[5]. Taylor,G.S and Gursul, I., "Buffeting flows over low sweep Delta wings", AIAA Journal, Vol.42, No.9,Sept. 2004, pp.1737-1745.

[6]. Yavuz, M.M, Elkhoury,M and Rockwell,D., "Buffeting flows over low sweep Delta wings", AIAA Journal, Vol.42, No.2,Feb. 2004, pp.332-340.

[7]. Luckring J M., "Reynolds Number, compressibility, and Leading-Edge Bluntness Effects on Delta Wing Aerodynamics", 24TH International Congress of The Aeronautical Sciences(ICAS), 2004.

[8]. Yanitepe B and Rockwell, D., "Flow structure on a Delta wing of low sweep angle", AIAA Journal, Vol.42, No.3, March. 2004, pp. 513-523.

[9]. Lin, J.C and Rockwell, D., "Transient structure of vortex breakdown on a Delta wing", AIAA Journal, Vol.33, No.1, Jan. 1995, pp.6-12.

[10]. Francis M. Payne, Terry Ng .T, and Robert C. Nelson., "Visualization of Leading Edge Vortices on a Series of Flat Plate Delta Wings", NASA Contractor Report 4320, 1991.

[11]. Gary E. Erickson., "Wind Tunnel Investigation of the Interaction and Breakdown Characteristics of Slender-Wing Vortices at Subsonic, Transonic, and Supersonic Speeds", NASA TP-3114, November 1991.

[12]. Gutmark Ephraim J and Guillot Stephen A., "Control of vortex breakdown over highly swept wings", AIAA Journal, Vol.43, No.5, Sept. 2005, pp.2065-2069.

[13]. Gursul I, Wang Z and Vardaki E., "Review of Flow Control Mechanisms of Leading-Edge Vortices", AIAA paper 2006-3508.

[14] J.J. Wang, Q.S. Li, J.Y. Liu, "Effect of vectored trailing jet on delta wing vortex breakdown", Experiments in fluids 34(2003) 651-654.

[15]. Russell M. Cummings, Scott A. Morton, and Stefan G. Siegel., "Computational Simulation and Experimental Measurements for a Delta Wing with Periodic Suction and Blowing", JOURNAL OF AIRCRAFT Vol. 40, No. 5, September–October 2003.

[16] Arne Henning, Markus Rutten, Claus Wagner and Markus Raffel, "A stereo PIV investigation of a vortex breakdown above a delta wing by analysis of vorticity field", AIAA 2005-4908.

[17] Robert Konrah, Christian Klein, Rolf H. Engler and Dirk Otter, "Analysis of PSP results obtained for the VFE-2 65° delta wing configuration at subsonic and transonic speeds", AIAA 2006-60.

[18]. Raju Channa and Viswanath. P R., "Pressure sensitive paint measurements in blow down wind tunnel", Journal of Aircraft, Vol.42, No.4,July-Aug 2005, pp.908-915.

[19]. Florent Renac, Didier Barberis, and Pascal Molton., " Control of Vortical Flow Over a Rounded Leading-edge Delta wing", AIAA JOURNAL,Vol. 43, No.7, July 2005.

[20]. Buddhadeb Nath., , "Flow Field Investigation Over a Delta Wing at Subsonic Speed", ME Thesis, .Department of Space Engineering and Rocketry, BIT, Mesra, Ranchi, 2007.

[21]. Martin V. Lowson., "Visualization measurements of vortex flows", JOURNAL OF AIRCRAFT , Vol. 28, No. 2, 1991.

[22]. B. Nath, S. Das and J. K. Prasad., "Investigation of flow field over blunted Delta wing", 3TH International Symposium on Applied Aerodynamics and Design of Aerospace Vehicles, SAROD-2007, Thiruvananthapuram

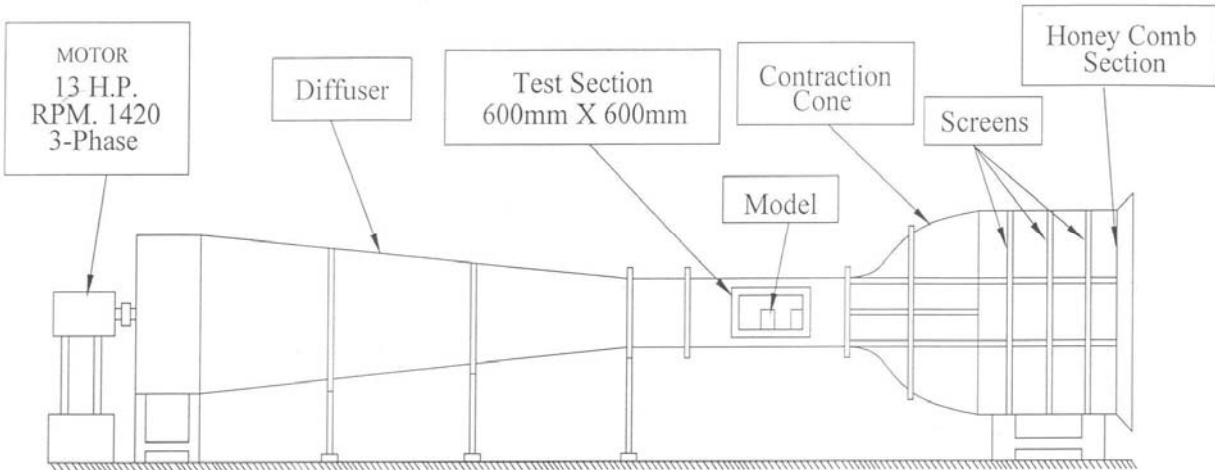

Fig. 1: A schematic sketch showing the details of the tunnel

Fig. 2: Photograph of low subsonic wind tunnel showing multi-tube manometer and pressure sensor

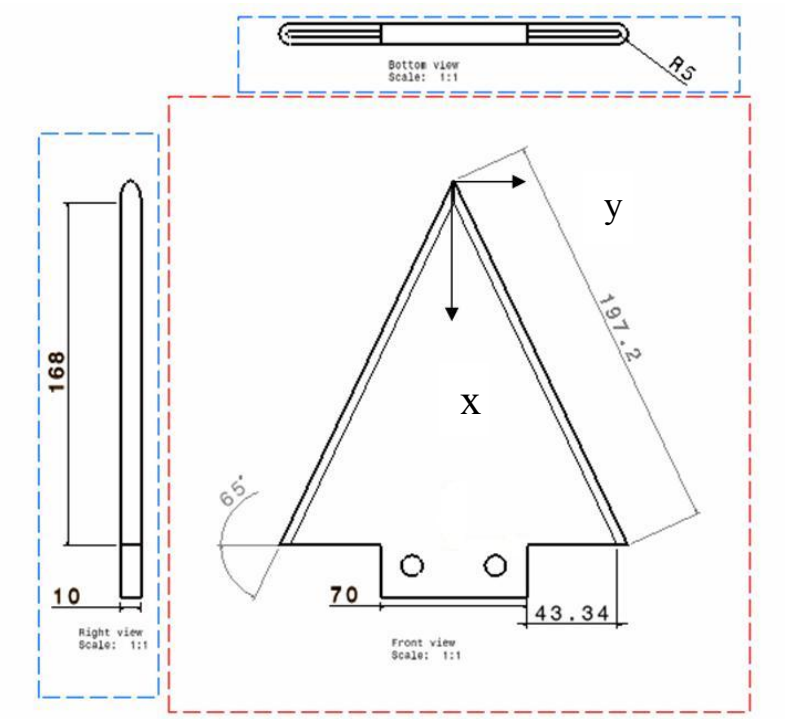

Fig. 3: Model details

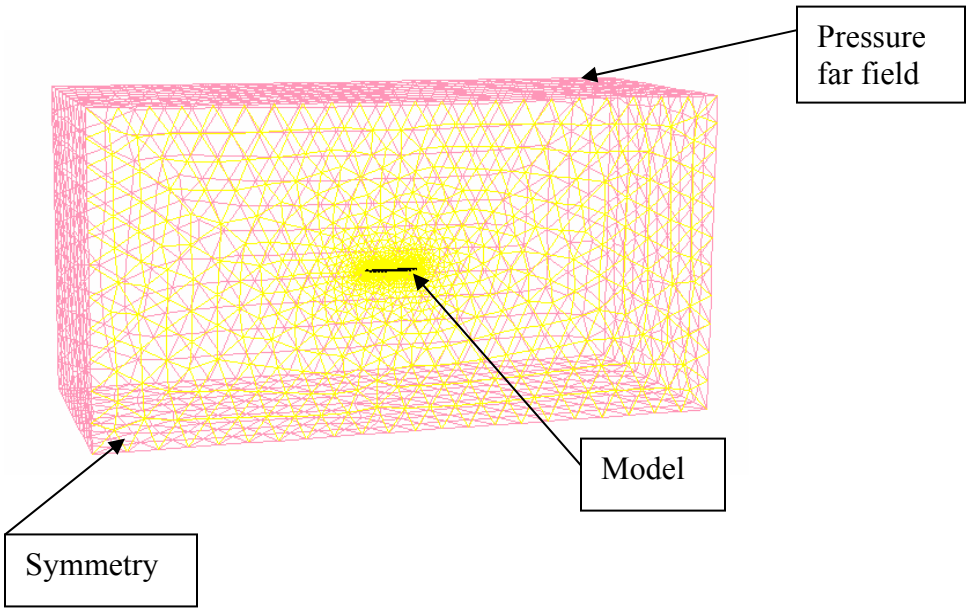

Fig 4: Overall grid distribution across the 3D flow

Fig 5: Tufts flow at α=20°, β=20°

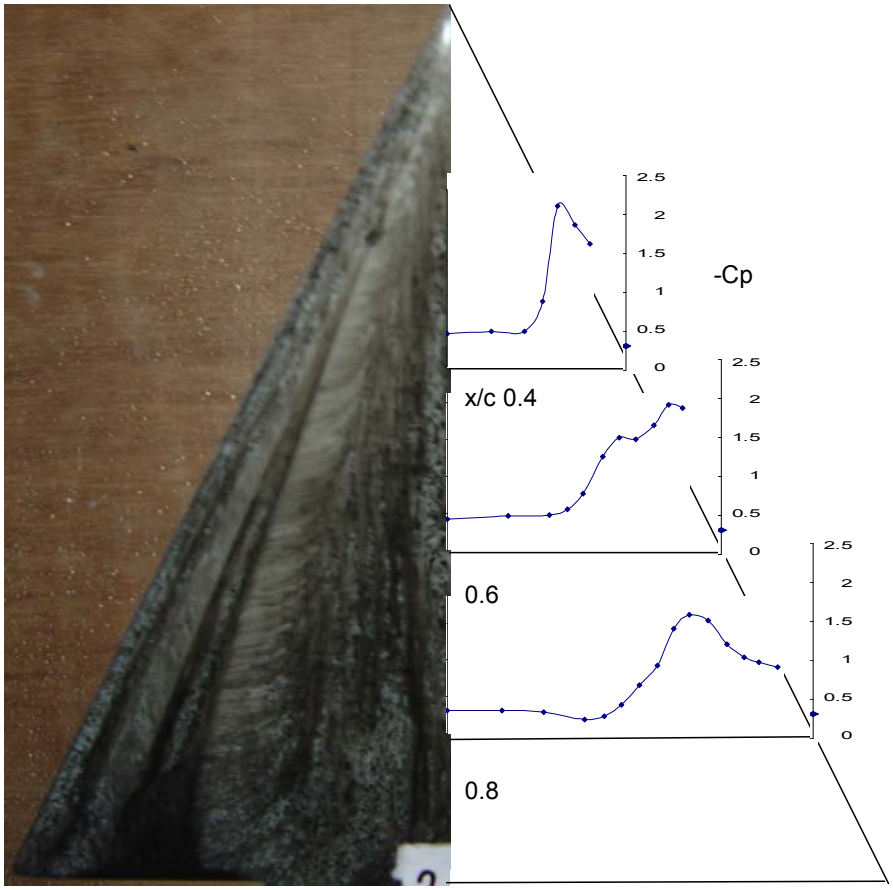

Fig 6: Oil flow visualization & Cp distribution at α=20°

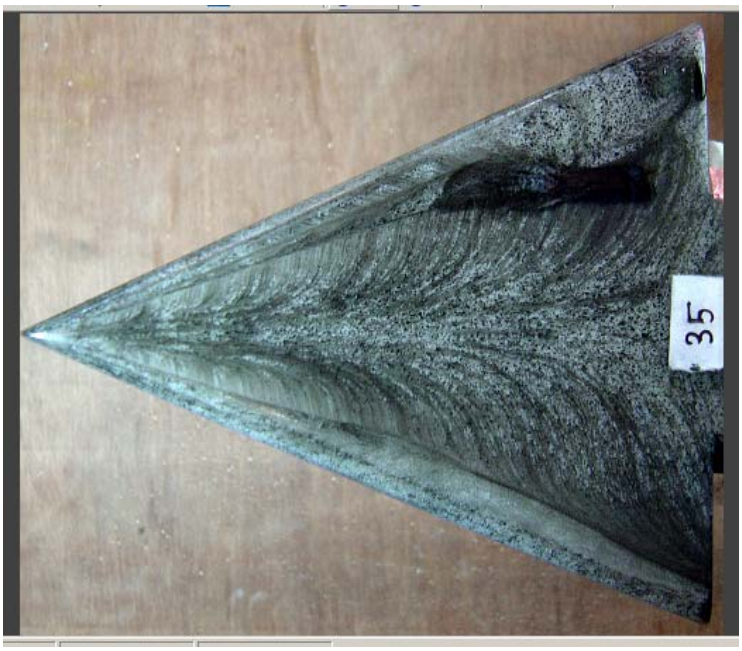

Fig 7: Oil flow visualization at α=35°

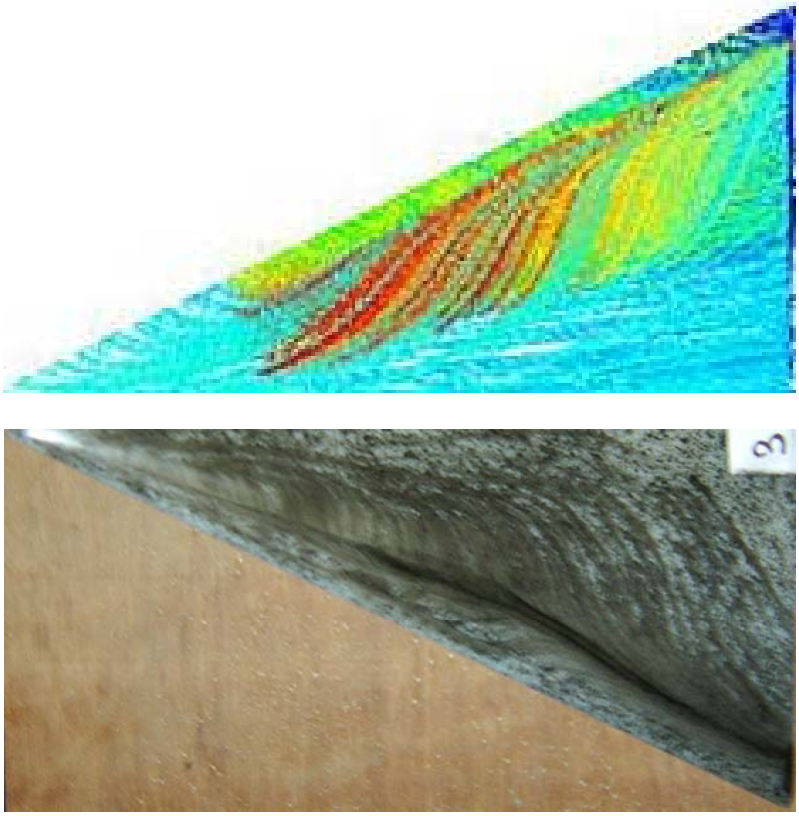

Fig.8: Comparison of computational oil flow and experimental oil flow

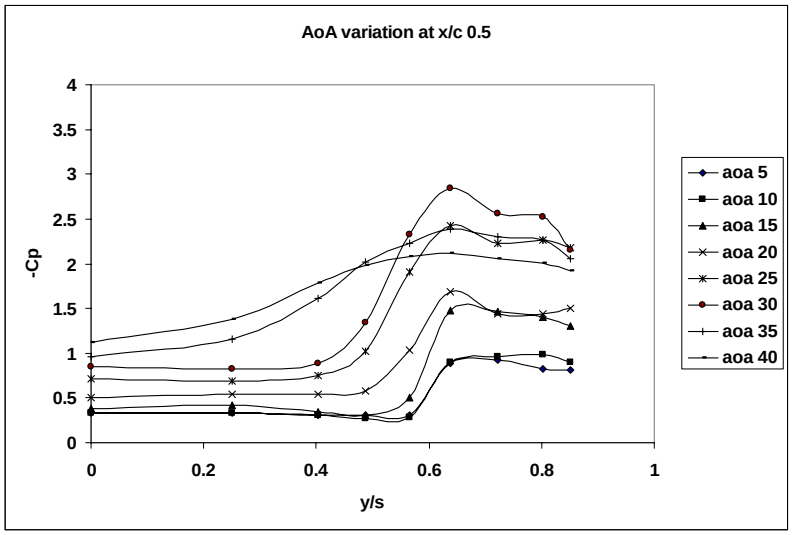

Fig 9: Cp distribution at x/c=0.5 at various angle of attack

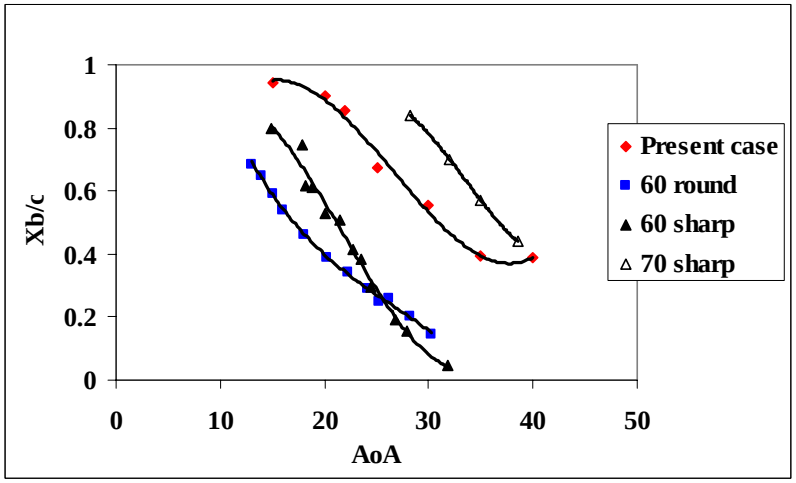

Fig. 10: Vortex breakdown location X_b/c vs angle of attack (α)

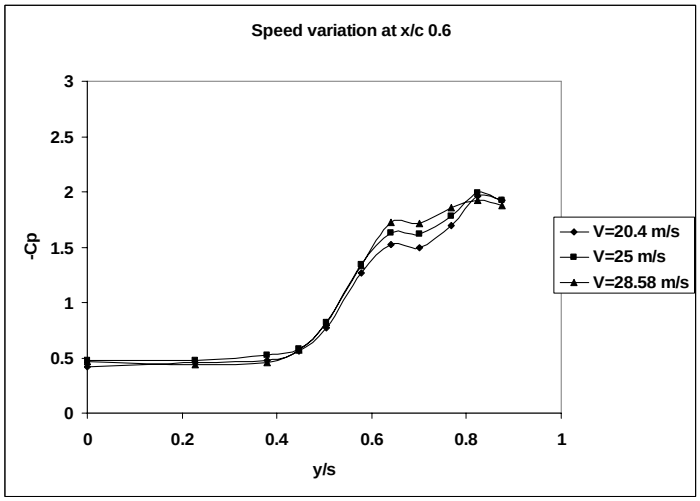

Fig. 11: Cp distribution at x/c=0.6 at various speeds

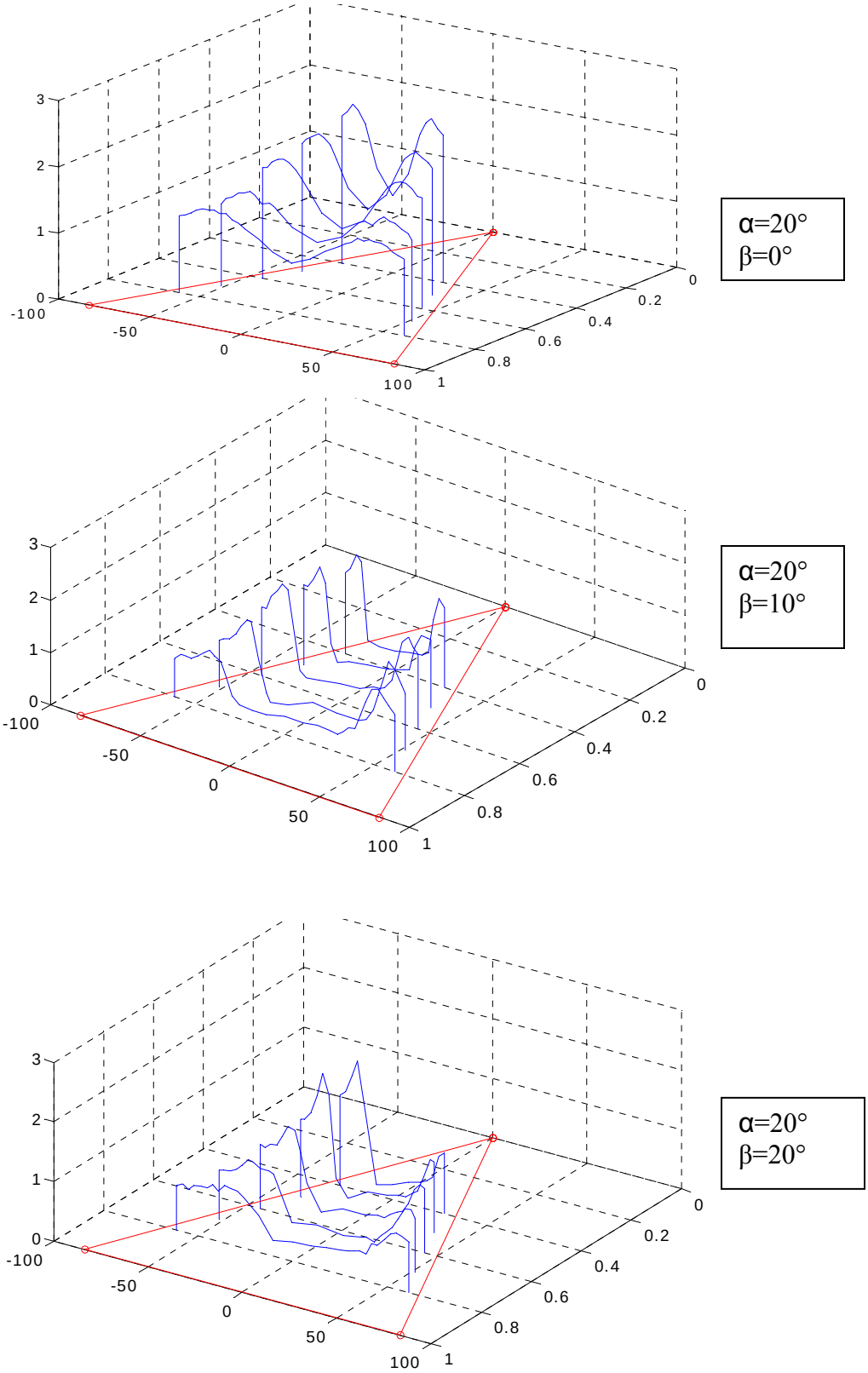

Fig. 12: Effect of β on leeward surface pressure distribution

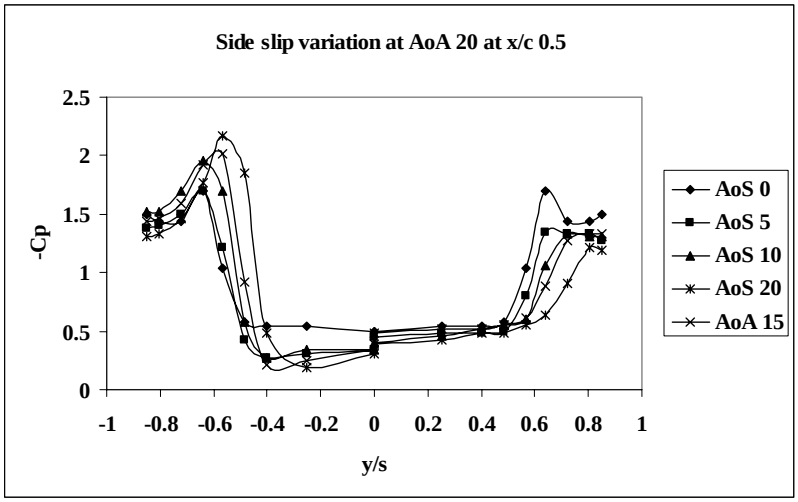

Fig. 13: Cp distribution at x/c=0.5 at various β

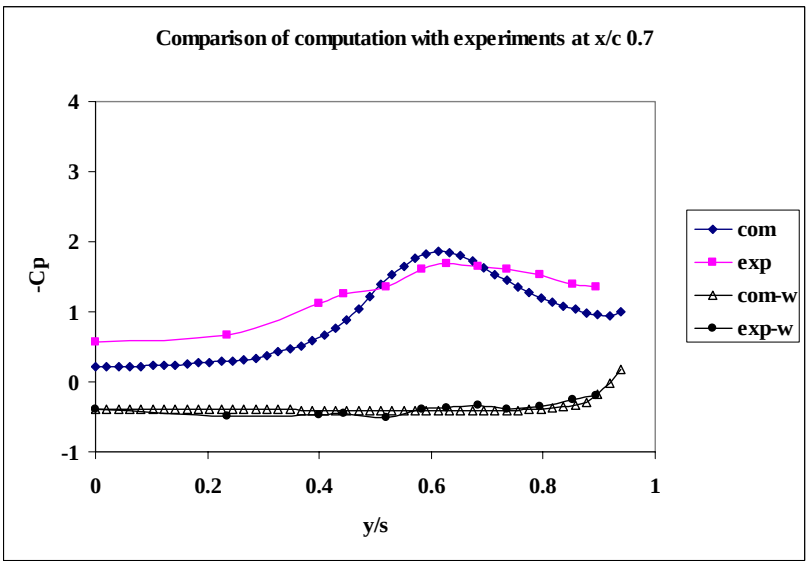

Fig. 14: Comparison of computed cp distribution with experimental data at x/c 0.7